Paper No.
10901

NACE INTERNATIONAL CORROSION Conference & Expo 2018

# OVERALL EFFECT OF VAPOR CORROSION INHIBITORS ON CASING CORROSION MITIGATION

Pavan K. Shukla(1)
Southwest Research Institute®
San Antonio, Texas, 78238
USA

Len J. Krissa
Enbridge Pipelines Inc.
10201 Jasper Ave NW
Edmonton, Alberta, T5J 3N7
Canada

Jerry DeWitt
Enbridge Energy Partners
222 US Highway 41, Suite 100,
Schererville, IN 46375
USA

## ABSTRACT

This work was conducted to evaluate effectiveness of the vapor corrosion inhibitors (VCIs) in the cased-crossing application. Specifically, the work was conducted to characterize electrochemical properties of two commercially available VCIs, and their effect on delivery of cathodic protection (CP) current to carrier pipe. Both experimental and modeling studies were conducted. Experimental studies were conducted with VCI gels, VCI only, and gel only solutions. Modeling was conducted to estimate the diversion of the CP current to casing when casing annuli are filled with the VCI gel solutions. It was found that the two commercially available VCIs performed well in the VCI gel formulations, and provided high level of corrosion protection to the carrier pipe inside the casing. In addition, both VCI gel formulations have low resistivity; therefore, a fraction of CP current could get diverted to the casing. This was confirmed in a large–scale testing. The diversion of the CP current needs to be analyzed on a case-by-case basis. The extent of CP current diversion was different for the two VCIs. It was noticed that one VCI formulation shifts the corrosion potential of the carrier pipe metal in the electronegative direction, as a result, the CP current demand and CP current diversion amounts are lower compared to other VCI formulation. The risk of hydrogen generation and accumulation due to diversion of the CP current through the casing was also evaluated. It was found that hydrogen generation commences even at the CP density of 1,000 mA/m$^2$. However, hydrogen effect is mitigated due to VCI gels' high viscosity, and their ability to buffer hydroxyl ions produced during the hydrogen evolution reaction.

Key words: Vapor Corrosion Inhibitors, Cased Crossings, Cathodic Protection, Hydrogen Generation.

---

(1) Current affiliation: Savannah River National Laboratory, Aiken, SC, 29808, pavan.shukla@srnl.doe.gov

## INTRODUCTION

A cased-pipeline segment is generally part of a longer pipeline. The carrier pipe is inside the casing in the segment, and is commonly referred as cased–crossing. The cased-crossings are used in geographical locations where the carrier pipes could be subject to variable mechanical loads, such as mechanical loadings due to vehicle passing on roadways. Casings provide mechanical protection to the carrier pipes. The cased pipe segments are generally safer compared to uncased pipelines because time-dependent threats, including third party excavation and miscellaneous external forces are largely eliminated.[1] However, a carrier pipe in a cased–crossing could be susceptible to external corrosion because of scenarios in which the annular space between carrier and casing becomes partly or completely filled with electrolyte. Such scenarios, as well as others, could cause accelerated corrosion of the carrier pipe.

Water-based VCI-gel formulations have been used in field to test the capability of VCI gel to mitigate external corrosion of the carrier pipe. Krissa et al.[2] tested the capability of vapor corrosion inhibitor (VCI) gel to control cased pipeline corrosion. The gel solution is prepared by mixing a VCI, potable water, and a gelling material. The gel is injected in casing annuli to mitigate corrosion of a carrier pipe that is under cathodic protection (CP). The gel is electrically conductive with ionic conductivity in the range of 0.1 to 0.5 Ohm-cm,[3] which could allow the carrier pipe inside the casing to receive the CP current. The work was conducted to characterize electrochemical properties of two commercially available VCIs, and to determine extent of CP current on a holiday inside the casing in presence of the either of the two commercially available VCIs in a cased–crossing.

Both experimental and modeling studies were conducted. Experimental studies were conducted with VCI gel, VCI only, and gel only solutions. Modeling was conducted to estimate the diversion of the CP current to casing when casing annuli are filled with the VCI gel solutions. This work reported in this paper is continuation of the previous study by Krissa et al. presented at CORROSION 2016. Some of the information in Krissa et al.[3] is reproduced for the sake of complete description and comparison of the experimental results reported in this paper.

## EXPERIMENTAL

Several corrosion cells were setup to test VCIs and their variations. Each corrosion cell was set up using the three-electrode configuration: (i) a working electrode, (ii) a counter electrode made of platinum-coated niobium wire mesh, and (iii) a saturated calomel reference electrode. The working electrode for each corrosion cell was prepared using 1 ft [30 cm] long and 2.375 inch [60 mm] diameter API(2) 5L X52 grade carbon steel pipe. One end of each pipe was sealed to avoid ingress of electrolyte inside the pipe. Only the exterior surface of the pipe was exposed to the electrolyte in each corrosion cell. Before each experiment, the electrode surfaces were sand blasted to expose the metal surface to the electrolyte. Sample images of the two working electrodes are presented in Figure 1. The electrode surfaces were also cleaned with the alcohol and DI water before using them in the corrosion cells.

1 gallon [3.79 L] size corrosion cells were used. A platinum (Pt)-coated niobium mesh was used as the counter electrode in all corrosion cells. The mesh specifications are following. Diameter of each wire in the mesh was 20 mils [0.508 mm] with Pt thickness of 0.1 mil [2.54 µm]. The mesh pattern was 10 × 10 wires/inch$^2$ [approximately 4 × 4 wires/cm$^2$] with an active surface area fraction of 1.25 in$^2$/in$^2$. An image of the counter electrode assembly along with its placement in the corrosion cell is shown in Figures 1(b) and 1(c). A saturated calomel electrode was used as the reference electrode for each corrosion cell. The reference electrode in each corrosion cell was brought in contact with the cell electrolyte using the Luggin probe.

---

(2) American Petroleum Institute (API) 1220 L St., N.W. Washington, DC 20005-4070

The VCI–based electrolytes for the corrosion cell were prepared according to mixing instructions provided by VCI vendors. Potable water was used as the mixing media for the VCIs, which consisted of vapor phase inhibitors and gelling materials. The two commercially available VCIs are identified as VCI A and VCI B. Each corrosion cell was connected to a potentiostat plus frequency response analyzer which was controlled through software. The working, counter, and reference electrodes were interfaced with a potentiostat for each corrosion cell.

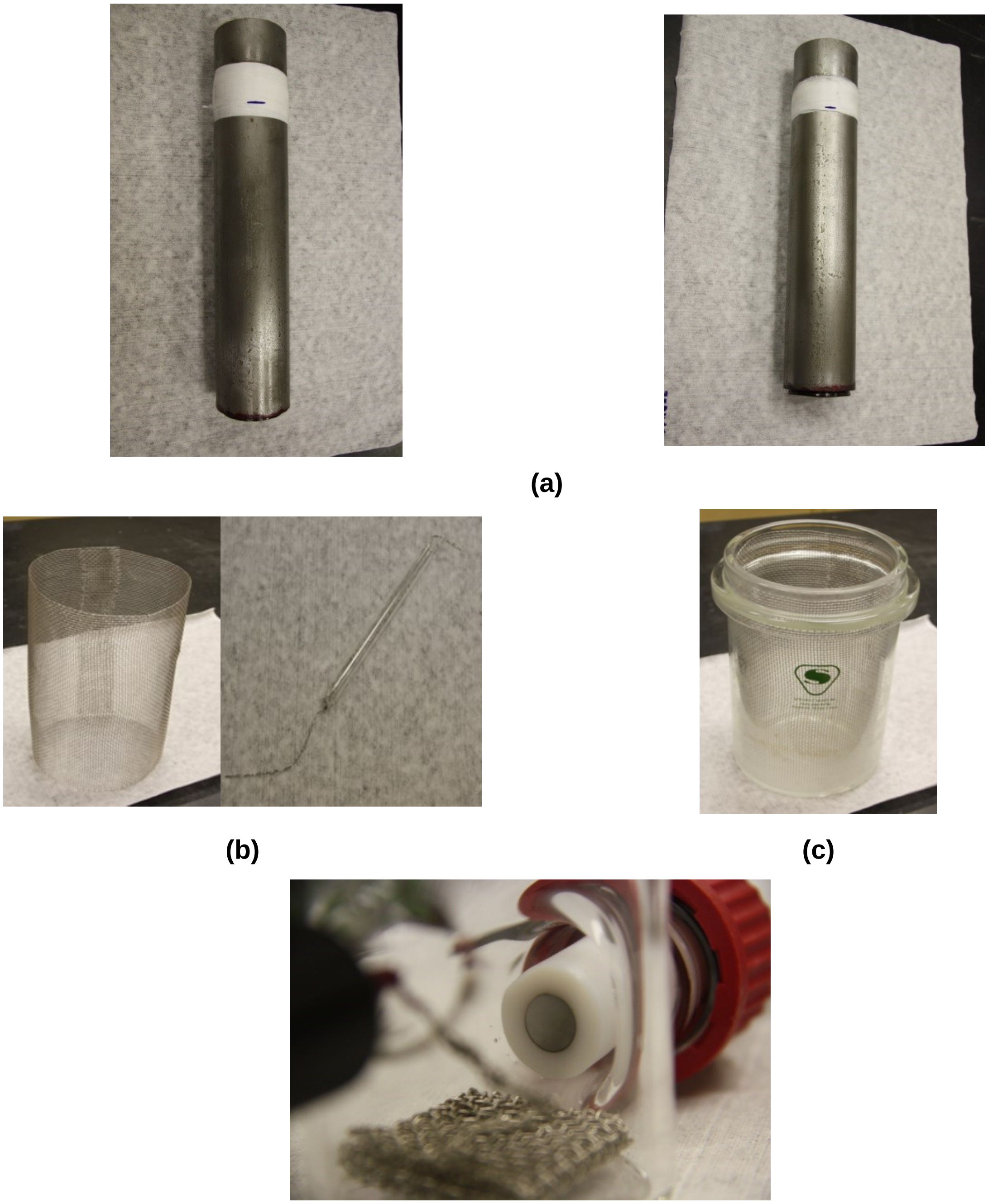

(a)

(b)

(c)

(d)

**Figure 1. (a) Images of the working electrodes used in corrosion cells; (b) counter electrode assembly; (c) counter electrode inside the corrosion cells; (d) working electrodes in the small–scale corrosion cells.**

Small-size corrosion cells, approximately 5.1 oz [150 ml], were used to accurately determine the effect of potentiostatic polarization on the native potential of the pipeline material. Images of the electrode assembly are presented in Figure 1(d). The diameters of the electrodes in the small-scale cell were 0.375 inch [9.5 mm].

## EXPERIMENTAL DATA AND RESULTS

### Open Circuit Potential

The open circuit potential data with respect to the saturated calomel electrode (SCE) for the electrodes in Figure 1(a) are presented in Figure 2. The data are from two repeat runs for each VCI. The data points with legends “VCI A (run 1)” and “VCI B (run 1)” are from Krissa et al.[3] As seen in the figure, the open circuit potential reached steady state after approximately 50 hours for the VCI A and 160 hours for VCI B. This indicated that it takes approximately 2–5 days for the pipe material to equilibrate with either of the two VCIs. The corrosion potential of the pipe material in VCI A is approximately −0.028 $V_{SCE}$. The corrosion potential of the pipe material in contact with VCI B ranged between −0.040 to −0.010 $V_{SCE}$. The corrosion potential data was reproducible for VCI A, but there was 60 mV difference between the two runs for VCI B.

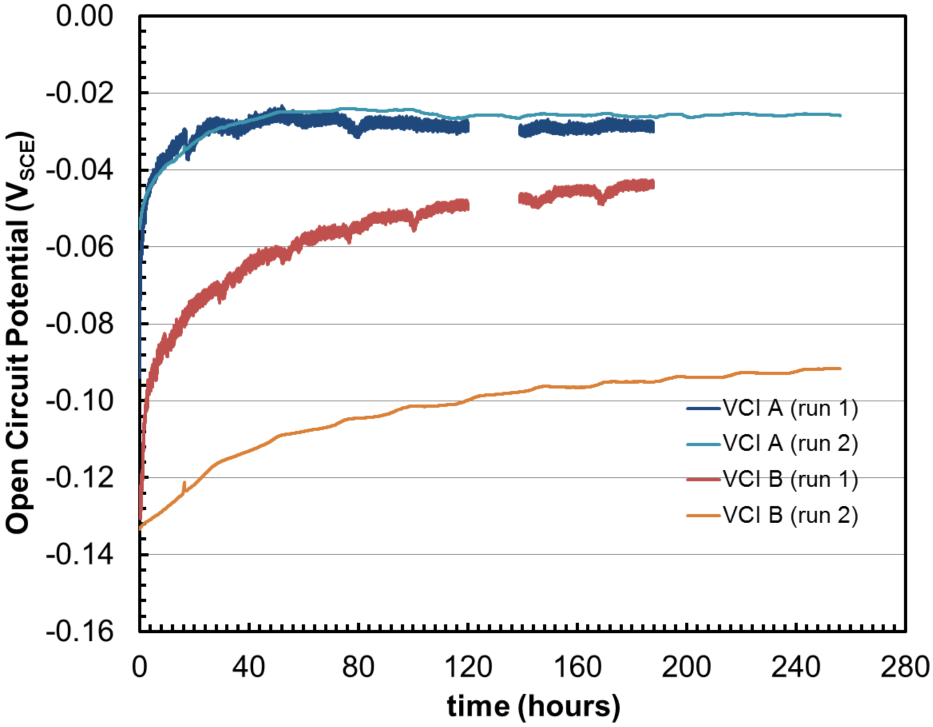

**Figure 2. Open circuit potential of the pipe material in contact with the two VCI gel solutions. Run 1 data, i.e., VCI A (run 1) and VCI B (run 1) gel solutions, for the two VCIs is from Krissa et al.[3]**

### Electrochemical Impedance Spectroscopy

After the corrosion potentials of the working electrodes stabilized and reached steady state, electrochemical impedance spectroscopy (EIS) was used to measure several impedance spectra of the working electrode in each corrosion cell. EIS data were used to estimate the corrosion rates. EIS is appropriate technique for this application because it allows measurement of very low corrosion rates. One or two EIS measurements were conducted per cell. The measurements were conducted at the open circuit potential of the corrosion cell and the data were used to estimate the polarization resistance. The EIS data were collected for VCI gel solutions (identified as VCI), VCI solutions prepared by mixing potable water and VCIs without the gelling materials (identified as VCI only), and solutions prepared by mixing potable water and gelling materials (identified as VCI gel only). The EIS data for the three sets of solutions are presented in Figure 3.

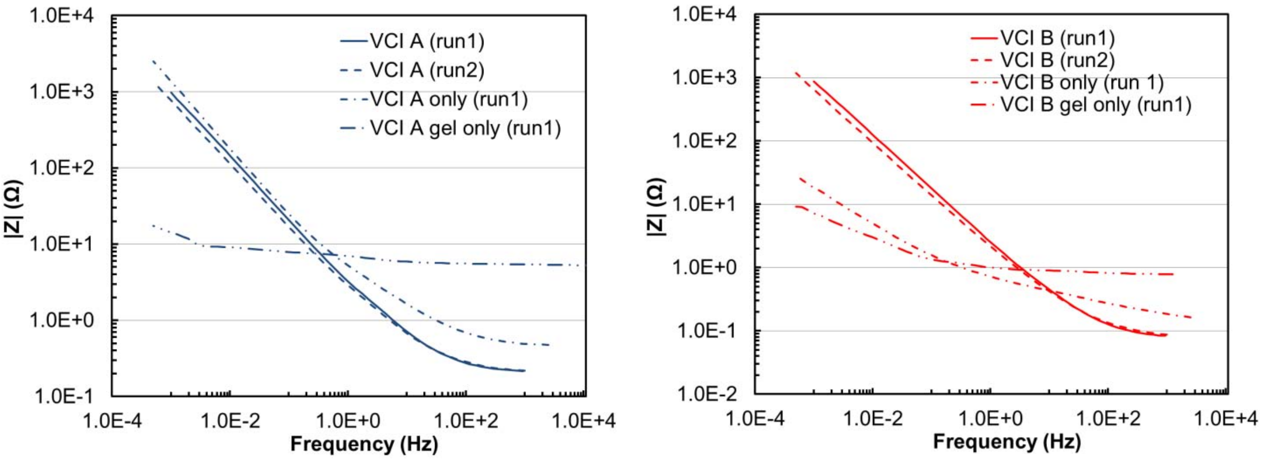

**(a)** **(b)**

**Figure 3. Bode plots of various variations of (a) VCI A and (b) VCI B. The VCI A and VCI B data is from Krissa et al.[3] VCI A and B: VCI gel solution, VCI A and B only: potable water + VCI, VCI A and B gel only: potable water + getting material.**

The impedance data were analyzed using a Randle type electrical circuit to obtain the polarization resistances. The analysis details are provided in Krissa et al.[3] The polarization resistances and corrosion rates are reported in Table 1. The corrosion rates of the pipe material in contact with both the VCI gel solutions (potable water + VCI + gelling material for each VCI) are in the sub-mil range. The corrosion rate for the VCI A only (solution without the gelling material) is also well below 1 mils/yr.

**Table 1. Polarization resistance values estimated from the circuit model fit to the impedance data and calculated corrosion rate of the electrode**

| Impedance Spectrum | Polarization Resistance (Ohm) | Corrosion Rate (mils/yr) |
|---|---|---|
| VCI A (run1)* | 10805.1 | $7.8 \times 10^{-3}$ |
| VCI A (run2)* | 8689.2 | $9.7 \times 10^{-3}$ |
| VCI B (run1)* | 13037.0 | $6.5 \times 10^{-3}$ |
| VCI B (run2)* | 9990.0 | $8.4 \times 10^{-3}$ |
| VCI A only (run1) | 20020 | $4.2 \times 10^{-3}$ |
| VCI B only (run2) | 50 | 1.68 |
| VCI A gel only (run1) | 20 | 4.21 |
| VCI B gel only (run1) | 19 | 4.43 |
| *Data are reproduced from Krissa et al.[3] | | |

## Potentiostatic Polarization Tests

Potentiostatic polarization curves were collected at five levels of potentials in both the VCIs. The working electrodes in both corrosion cells were polarized at a set potential for approximately 120 hours. The current between the working (pipe cathode) and counter (anode) electrodes was measured. The current versus time curves in Figure 4(a) were measured at −675, −775, −875, −975, and −1,075 $mV_{SCE}$ polarization levels for VCI A. As seen in Figure 4(a), the current reached steady–state in approximately 24 hours after polarization. In addition, the steady–state current is cathodic (i.e., negative) for the polarization levels, indicating that dominant electrochemical reaction at the electrode surface is reduction of certain species. For −675 mV$_{SCE}$ polarization level, a small amount of oxidizing current is noted immediately after polarization. However, the oxidizing current subsided within 8 hours, and became cathodic afterwards. Further, the magnitude of the oxidizing current is less than 0.4 mA. The current versus time data for VCI B are presented in Figure 4(b). The curves in Figure 4(b) also were measured at −675, −775, −875, −975, and −1,075 mV$_{SCE}$ polarization levels. For −675 and −775 mV$_{SCE}$ polarization levels, a larger amount of oxidizing current is noted immediately after polarizing the working electrode in VCI B compared to VCI A. The peak oxidizing currents are approximately 20 and 12 mA for −675 and −775 mV$_{SCE}$ polarization levels, respectively. Figures 5(a) and 5(b) show the rest potentials after 120 hours of polarization for VCI A and VCI B, respectively. The of rest potentials indicate that surface characteristics of the electrodes change due to VCIs. The steady–state values rest potentials are corrosion potentials. The corrosion potential of the pipe material decreased by 730 mV due to polarization in VCI A compared to the open circuit potential (OCP) of −28 mV$_{SCE}$ in Figure 2, whereas the corrosion potential of the pipe material somewhat increased due to polarization in VCI B when compared to OCP of −40 to −10 mV$_{SCE}$ in Figure 2.

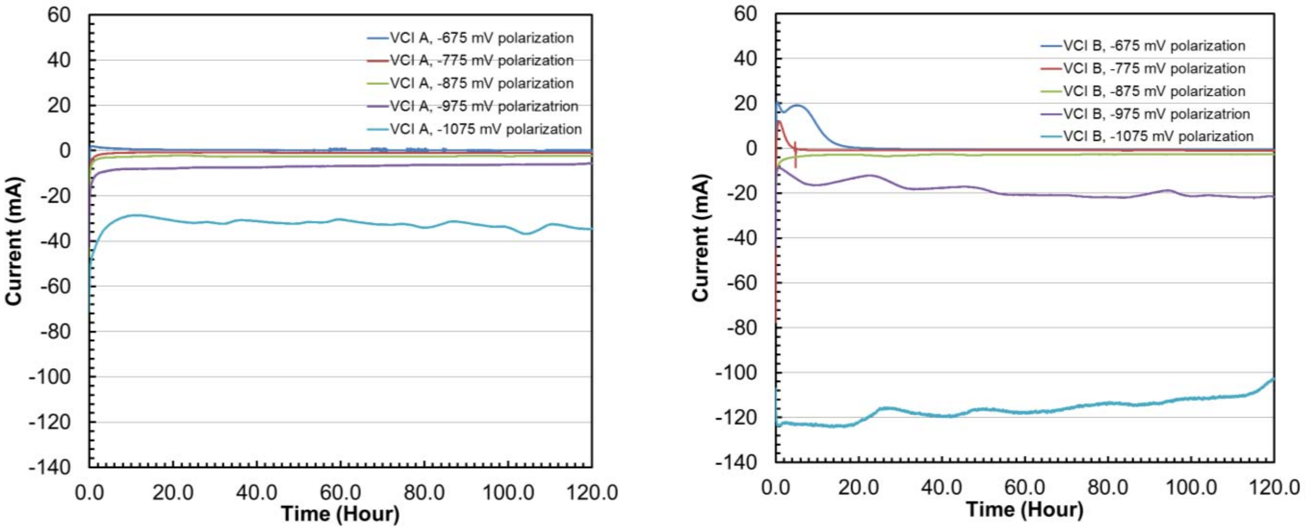

(a) (b)

**Figure 4. Potentiostatic polarization current of working electrode in contact with (a) VCI A, and (b) VCI B gel solutions**

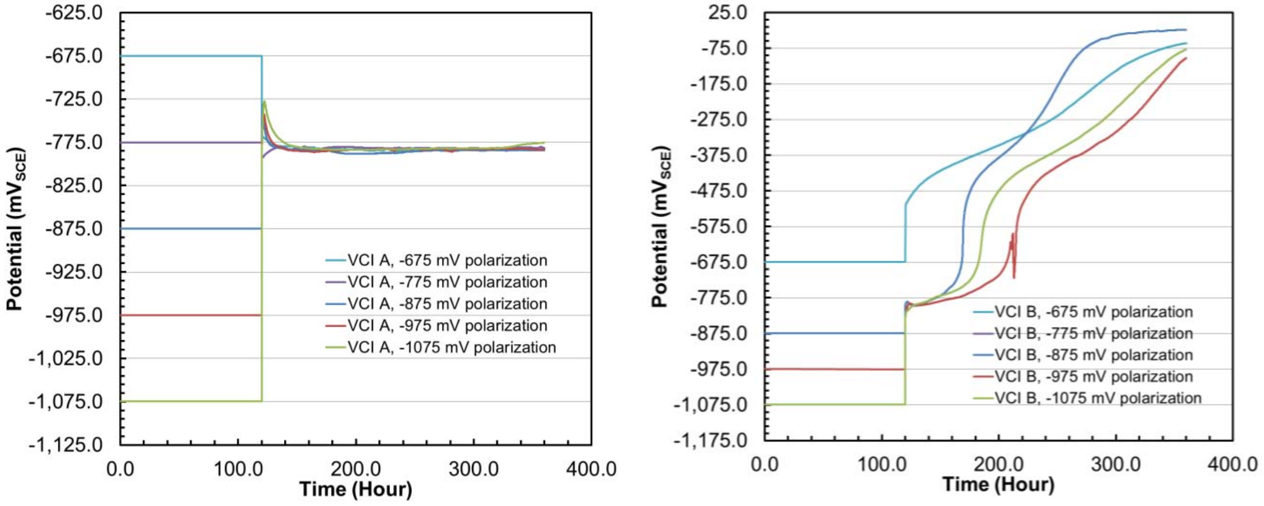

**(a) (b)**

**Figure 5. Rest potential measurement after potentiostatic polarization for 120 hours for (a) VCI A and (b) VCI B gel solutions**

### CP Current Demand

The CP current demands at various polarization levels are listed in Table 2. The current densities were calculated by normalizing the current value with the surface area of pipe electrode, 60 in$^2$ ($385 \times 10^{-4}$ m$^2$). The listed data show that the current density demand for polarizing the pipe surface is somewhat lower in VCI A compared to VCI B. In addition, as seen in Figure 4(b), VCI B has chemical components that could exhibit oxidation when subjected to cathodic polarization. However, this phenomenon is temporary and declines after initial consumption of the components in VCI B chemistry.

**Table 2. Steady-state current density for various polarization levels**

| Polarization Level ($mV_{SCE}$) | VCI gel solutions current density (mA/m$^2$) | | VCI only current density (mA/m$^2$) | | Gel only current density (mA/m$^2$) | |
|---|---|---|---|---|---|---|
| | VCI A | VCI B | VCI A | VCI B | VCI A | VCI B |
| −675 | −0.2 | −16.6 | 37.1 | −12.5 | −10.6 | −46.7 |
| −775 | −16.2 | −20.1 | −11.8 | 319.4 | −20.3 | −129.3 |
| −875 | −32.5 | −56.0 | −73.0 | −66.7 | −71.4 | −195.8 |
| −975 | −76.1 | −548.2 | −324.6 | −597.2 | −118.9 | −280.2 |
| −1,075 | −2,189.6 | −2,274.2 | −1,264.6 | −3,583.5 | −263.6 | −404.8 |

## MODELING

### Model Description

The model equations are described in depth in previous works by Song et al. and Shukla et al.[4-6] The model details are briefly discussed for the sake of completeness. A schematic representing a coated carrier pipe and casing is presented in Figure 6.

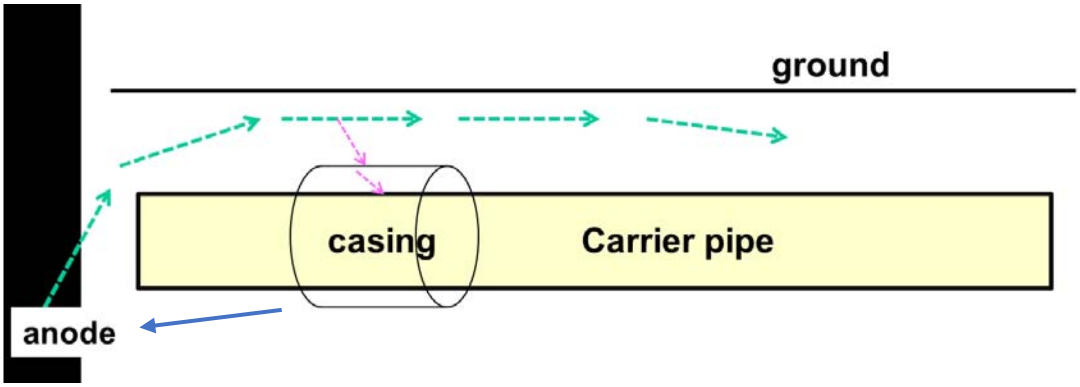

**Figure 6. Schematic of the carrier and casing pipe. Green and pink arrows show flow of CP current to the pipe and casing, and blue arrow shows return current.**

Potential distribution in the soil domain outside the casing is governed by:

$$\frac{1}{\rho_{soil}} \nabla^2 \varphi_{soil} = 0 \qquad (1)$$

similarly, the potential distribution inside the casing is governed by

$$\frac{1}{\rho_{annulus}} \nabla^2 \varphi_{annulus} = 0 \tag{2}$$

where

$\varphi_{soil}$ — soil potential at the carrier and casing pipes and soil interface (V) with respect to Cu/CuSO$_4$ electrode
$\varphi_{annulus}$ — electrolyte potential at the casing and electrolyte interface in annulus (V) with respect to Cu/CuSO$_4$ electrode
$\rho_{soil}$ — soil resistivity (Ω-m)
$\rho_{annulus}$ — resistivity of the electrolyte in annulus (Ω-m)

When a casing annulus is filled with a given vapor corrosion inhibitor (VCI) gel, the electrolytic coupling is established between the carrier and the casing pipe. In the case of electrolytic contact between the casing and the carrier pipe, the total current that flows across the two surfaces of the casing wall must be equal to

$$I_{cs,soil} = -I_{cs,annulus} \tag{3}$$

where $I_{cs,soil}$ is the total current entering the casing wall from the soil side and $I_{cs,annulus}$ is the total current leaving the casing wall at the annulus side. $I_{cs,soil}$ is given by

$$I_{cs,soil} = \int i_{corr,soil} \left[ 10^{\frac{\psi_c - \varphi_{soil} - E_{corr,soil}}{b_{Fe}}} - 10^{\frac{-(\psi_c - \varphi_{soil} - E_{corr,soil})}{b_{H_2O}}} \right] dS_{external} \tag{4}$$

where

$i_{corr,soil}$ — current density at the casing and soil interface (A/cm$^2$)
$E_{corr,soil}$ — corrosion potential of the casing at the soil interface (V)
$\psi_c$ — casing wall metal potential (V) with respect to Cu/CuSO$_4$ electrode
$b_{Fe}, b_{H2O}$ — Tafel slope for iron oxidation and water reduction reaction, respectively (V/decade)
$S_{external}$ — external surface area of casing wall (m$^2$)

The expression on the right-hand side of Eq. (4) is simplified using linearization of Butler-Volmer equation according to following:

$$I_{cs,soil} = \int \frac{\psi_c - \varphi_{soil} - E_{corr,soil}}{Rp_{cs,soil}} dS_{external} \tag{5}$$

where

$$Rp_{cs,soil} = \frac{B}{i_{corr,soil}}, \; B = \frac{b_{Fe} b_{H2O}}{2.303(b_{Fe} + b_{H2O})} \tag{6}$$

$Rp_{cs,soil}$ is the polarization resistance (Ω-m$^2$) of the casing wall at the casing and soil interface. Similarly, $I_{cs,annulus}$ is given by

$$I_{cs,annulus} = \int \frac{\psi_c - \varphi_{annulus} - E_{corr,annulus}}{Rp_{cs,annulus}} dS_{internal} \qquad (7)$$

where

$E_{corr,annulus}$ — corrosion potential of the casing at the electrolyte interface in casing (V)
$Rp_{cs,annulus}$ — polarization resistance (Ω-m$^2$) of the casing wall at the casing and electrolyte interface in annulus (Ω-m$^2$)
$S_{internal}$ — internal surface area of casing wall (m$^2$)

Equations (6) and (7) are substituted in Eq. (3), and under assumption that the metal potential is constant, the following expression is obtained for average casing wall metal potential

$$\psi_c = \frac{\left[\left(\varphi_{annulus} + E_{corr,annulus}\right)Rp_{cs,soil}S_{internal} + \left(\varphi_{soil} + E_{corr,soil}\right)Rp_{cs,annulus}S_{external}\right]}{Rp_{cs,annulus}S_{external} + Rp_{cs,soilS_{internal}}} \qquad (8)$$

$\psi_c$ in Eq. (8) is used to estimate the local current density at the casing and soil interface according to the following expression

$$i_{cs,soil} = \frac{\psi_c - \varphi_{soil} - E_{corr,soil}}{Rp_{cs,soil}} \text{ and } i_{cs,annulus} = \frac{\psi_c - \varphi_{annulus} - E_{corr,annulus}}{Rp_{cs,annulus}} \qquad (9)$$

The boundary conditions for the coated pipe outside the casing for the coated pipe inside the annulus are given by

$$i_{coated,soil} = \frac{V_m - \varphi_{soil} - E_{corr\_coated,soil}}{Rp_{coat}} \text{ and } i_{coated,annulus} = \frac{V_m - \varphi_{annulus} - E_{corr\_coated,annulus}}{Rp_{coat}} \qquad (10)$$

where
$i_{coated,soil}$ — current density at coated part of the carrier pipe and soil interface outside the casing (A/cm$^2$)
$V_m$ — metal potential of the carrier pipe (V)
$E_{corr\_coated,soil}$ — corrosion potential of the coated carrier pipe at the soil interface (V)
$E_{corr\_coated,annulus}$ — corrosion potential of the coated carrier pipe at the pipe and casing solution interface (V)
$\psi_c$ — casing wall metal potential (V) with respect to $Cu/CuSO_4$ electrode
$Rp_{coat}$ — polarization resistance (Ω-m$^2$) of the coating both outside and inside the casing (Ω-m$^2$)

The boundary condition for the holiday inside the casing is given by

$$i_{holiday,annulus} = \frac{V_m - \varphi_{annulus} - E_{holiday,annulus}}{Rp_{hoilday,annulus}} \qquad (11)$$

where
$i_{holiday,annulus}$ — current density at holiday surface inside the casing (A/cm$^2$)
$E_{holiday,annulus}$ — corrosion potential of the holiday inside the casing electrolyte interface (V)
$Rp_{hoilday,annulus}$ — polarization resistance (Ω-m$^2$) of the holiday inside the casing at the casing solution and metal surface interface

## Model Results

The model was simulated for an impressed current CP system; the current output from anode array was estimated using external surface area of the pipe. The model was simulated for the fusion bonded epoxy coating; however, it can be easily modified to simulate other coating types. The current output from anode array was based on the CP current demand of the fusion bonded epoxy coated pipe being equal to 0.9 mA/m$^2$ for 30 year life.[7] The model parameter values are listed in Table 3.

The model results are presented for a 22 inch [55.9 cm] pipe with a 26 inch [66.0 cm] casing. A 1.6 in$^2$ [10 cm$^2$] holiday was modeled on the carrier pipe inside the casing. The holiday was located at the 9 O'clock location, facing towards the anode bed. The effects of coating and changes in pipe and casing dimensions on the current distributions are described. CP current distributions on the pipeline with the two VCIs are presented next.

**Table 3. Parameter values used to simulate the model**

| Parameter | Value | |
|---|---|---|
| | VCI A | VCI B |
| **Pipe-soil parameters:** | | |
| $\rho_{soil}$ | 25 Ω–m | 25 Ω–m |
| $Rp_{coat}$ | 5,000 Ω–m$^2$ | 5,000 Ω–m$^2$ |
| $E_{corr\_coated,soil}$ | −550 $mV_{CSE}$ | −500 $mV_{CSE}$ |
| **Casing-soil parameters:** | | |
| $Rp_{cs,soil}$ | 5 Ω–m$^2$ | 5 Ω–m$^2$ |
| $E_{corr,soil}$ | −600 $mV_{CSE}$ | −600 $mV_{CSE}$ |
| **Casing-annulus and pipe-annulus parameters:** | | |
| $\rho_{annulus}$ | 0.15 Ω–m | 0.5 Ω–m |
| $E_{corr,annulus}$ | −110 $mV_{CSE}$ | −120 $mV_{CSE}$ |
| $Rp_{cs,annulus}$ | 400 Ω–m$^2$ | 400 Ω–m$^2$ |
| $E_{corr\_coated,annulus}$ | −550 $mV_{CSE}$ | −550 $mV_{CSE}$ |
| $E_{holiday,annulus}$ | −110 $mV_{CSE}$ | −750 $mV_{CSE}$ |
| $Rp_{hoilday,annulus}$ | 0.3 Ω-m$^2$ | 0.3 Ω-m$^2$ |
| **Pipe, casing, and anode parameters** | | |
| Pipe diameter | 22 inch [55.9 cm] | 22 inch [55.9 cm] |
| Casing diameter | 26 inch [66.0 cm] | 26 inch [66.0 cm] |
| Pipe length | 7.46 mile [12 km] | 7.46 mile [12 km] |

### VCI A

The pipe current density data are presented in Figures 7(a) and 7(b). The current density at the holiday on the carrier pipe inside the casing is shown in Figure 8(a). The current density at the holiday is approximately equal to 14,000 mA/m$^2$. This current density is relatively high and could lead to formation and accumulation of hydrogen in the VCI gel solution.

### VCI B

The pipe current density data are presented in Figures 9(a) and 9(b). The current density at the holiday surface on the carrier pipe inside the casing is shown in Figure 8(b). As seen in Figure 8(b), the current density at the holiday is approximately equal to 16,000 mA/m$^2$. The current density at the holiday for VCI B is higher than the VCI A.

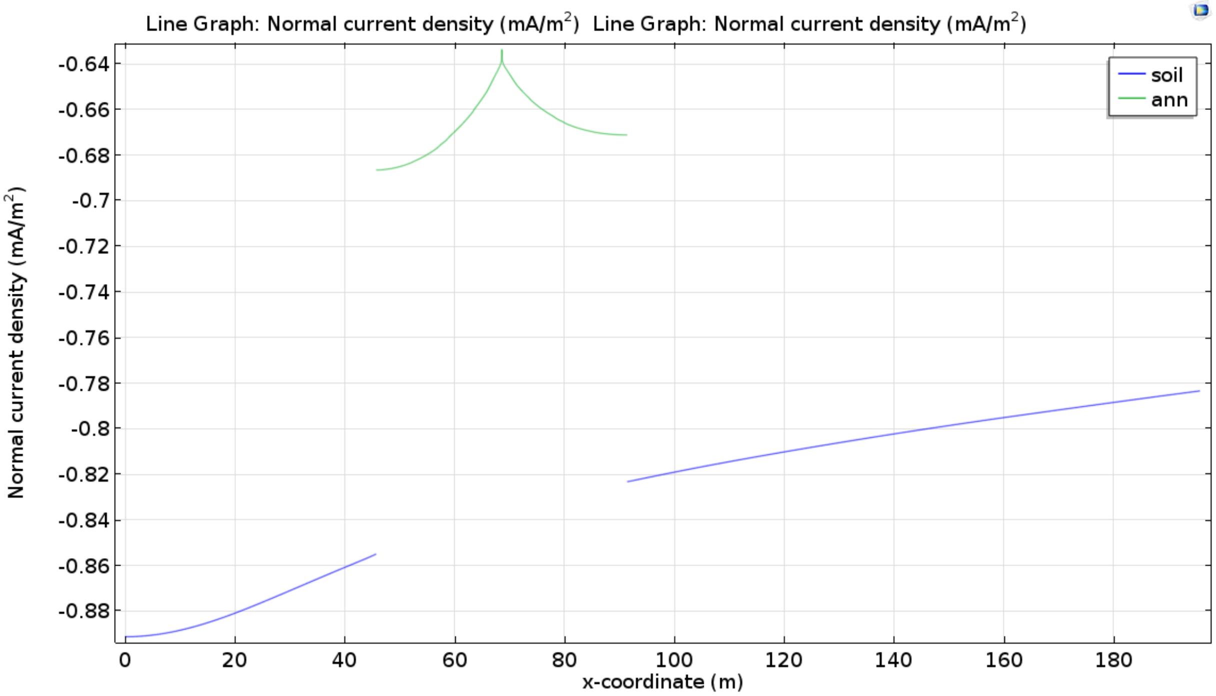

**(a) Around the casing**

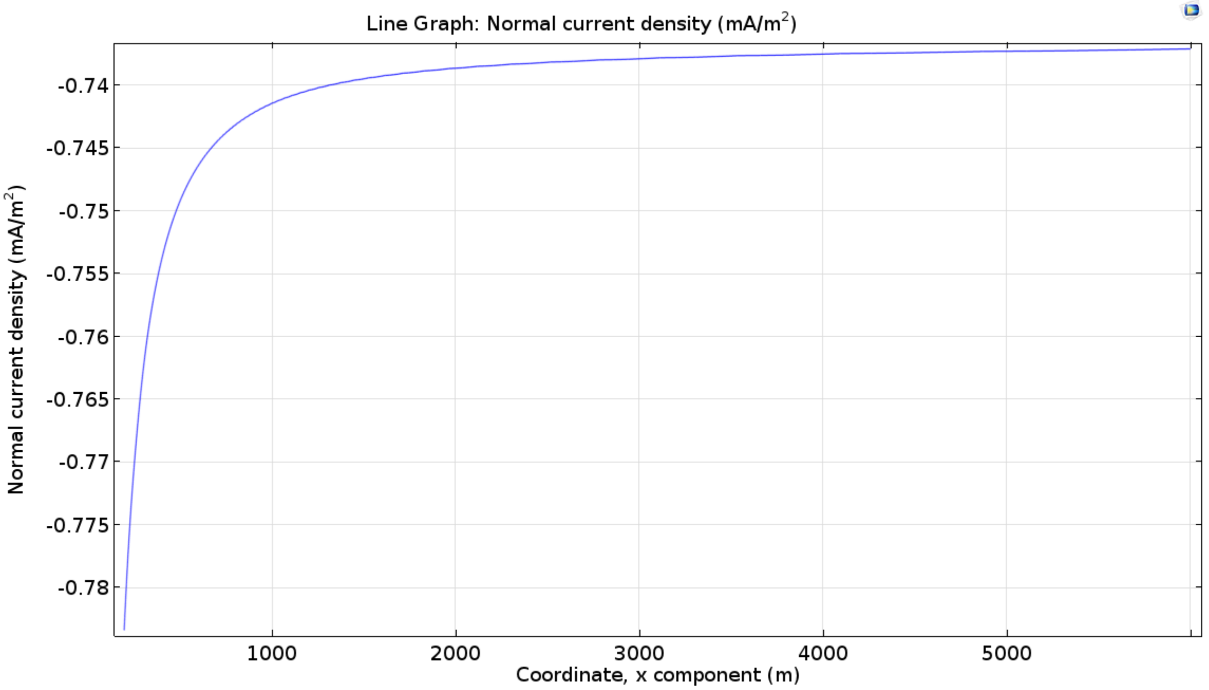

**(b) Away from the casing**

**Figure 7. Pipe current density for VCI A: (a) around the casing and (b) away from the casing**

The following explanation is provided for the holiday current density being higher for VCI B than VCI A. The corrosion potential of the metal surface shifts in the electronegative direction due to exposure to

VCI A compared to OCP, whereas the corrosion potential of the metal shifts in electropositive direction due to exposure to VCI B compared to OCP. As a result, the holiday CP current density is lower in VCI A compared to VCI B. Nonetheless, the current densities at the holiday for both the VCIs are high which could lead to hydrogen generation at the holidays and subsequent accumulation of hydrogen in the VCI gels.

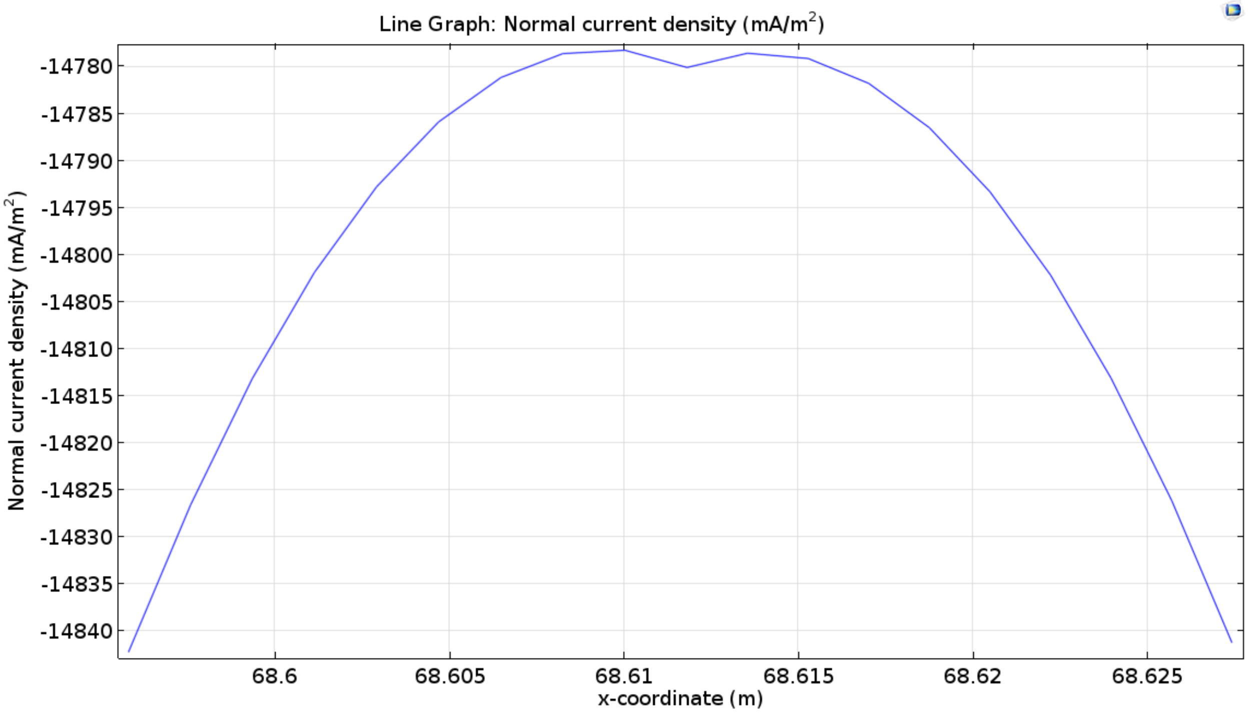

**(a) Holiday current density for VCI A**

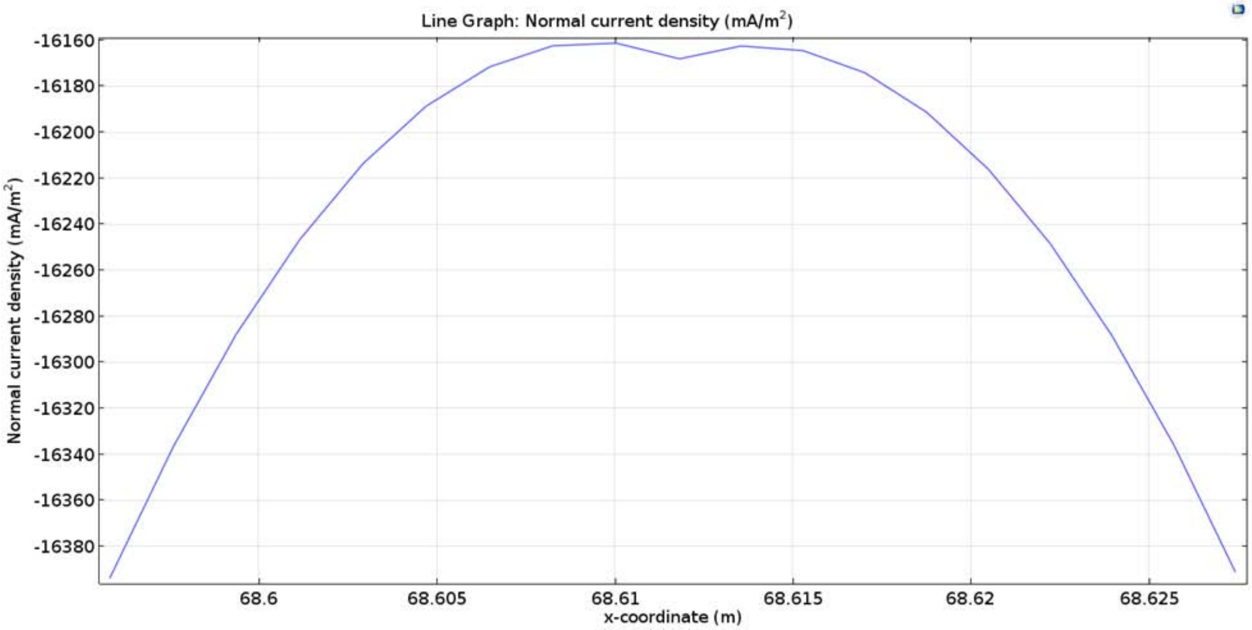

**(b) Holiday current density for VCI B**

**Figure 8. Holiday current density for (a) VCI A, and (b) VCI B**

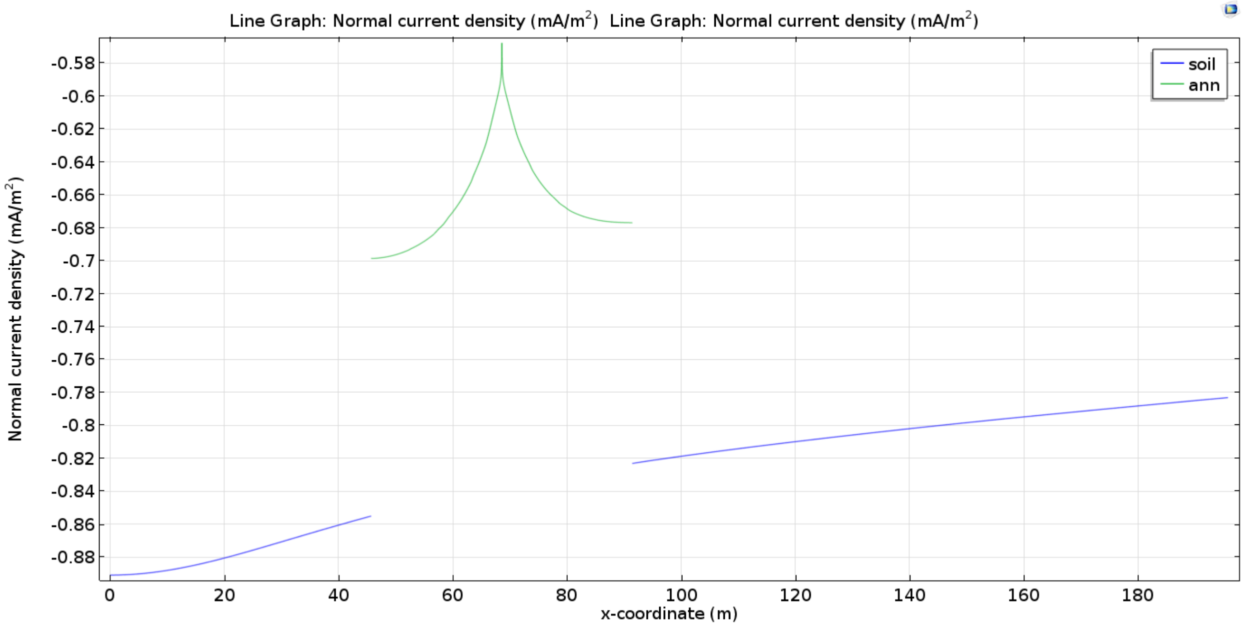

**(a) Around the casing**

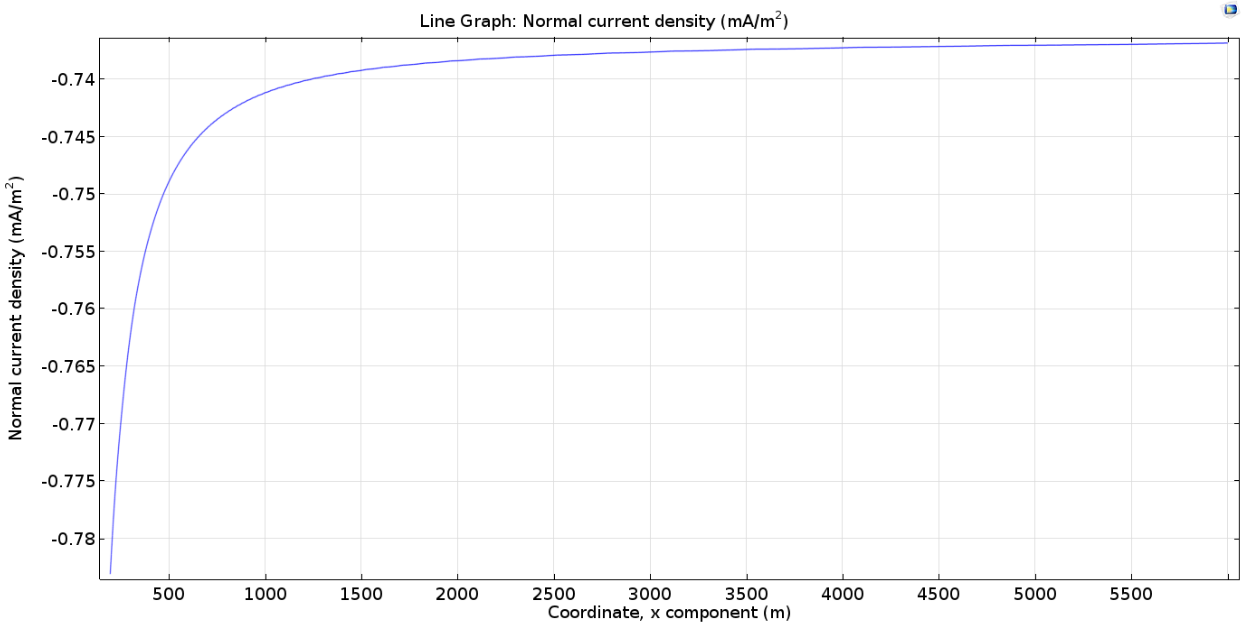

**(b) Away from the casing**

**Figure 9. Pipe current density for VCI B: (a) around the casing and (b) away from the casing**

## SUMMARY

The experimental studies provide data to support that both VCI A and VCI B perform well in the vendor-recommended gel formulations. Both VCIs provide a very high level of corrosion protection to the carrier pipe inside the casing. The VCI A only formulation, i.e., VCI A solution prepared by mixing potable water plus inhibitor (without the gelling material) also provides a high level of protection against corrosion. This was not the case with the VCI B only solution. Both VCI gel formulations have low resistivity; therefore, a fraction of cathodic protection (CP) current could get diverted to the casing. This was confirmed in the large–scale testing which is reported elsewhere.[8] The diversion of the CP current in a VCI gel filled casing needs to be analyzed on a case-by-case basis. It is, however, noted that VCI A shifts the corrosion potential of the metal in the electronegative direction with respect to the open circuit potential, as a result, the CP current demand and CP current diversion amounts are lower compared to VCI B. Hydrogen generation commences even at the current density of 1,000 mA/m$^2$.[8] The intensity of the hydrogen generation increases with increasing current densities.[8] The modeling results indicate that there is no practical limit on the cathodic current density at the holiday surfaces inside a casing filled with VCI gel. Effect of hydrogen generation was found to be mitigated by VCI gels' high viscosity, and their ability to buffer hydroxyl ions produced during the hydrogen evolution reaction.

## ACKNOWLEDGEMENTS

The authors would like to recognize and sincerely thank Enbridge Pipelines' Mike Hill, Yvan Hubert, Kurt Baraniecki and Walter Kresic for their continual support, dedication and devotion towards advancing pipeline integrity management.

## REFERENCES

1. Southwest Research Institute, "Statistical Analysis of External Corrosion Anomaly Data of Cased Pipe Segments," INGAA Foundation, Report No. F-2007-10, December 2007.

2. L.J. Krissa, J. Dewitt, and T. Whited. "Development and Application of a New Solution for Mitigation of Carrier Pipe Corrosion Inside Cased Pipeline Crossings," CORROSION/2014, paper no. 4167 (Houston, TX, NACE, 2014).

3. L.J. Krissa, J. Dewitt, and P.K. Shukla, "Experimental Studies to Determine Effects of Vapor Corrosion Inhibitors for Mitigating Corrosion in Casing," CORROSION/2016, paper no. C2016-7801 (Houston, TX, NACE, 2016).

4. F.M. Song, A. Nordquist, and P. Shukla, "Large-Scale Model Developed for Predicting the Carrier Pipe Potential inside a Metallic Casing," Corrosion, Vol. 69, No. 12 (2013): p. 1180.

5. P.K. Shukla, A. Nordquist, and F. Song, "Development of Cased-Pipeline Corrosion Model and Its Validation With Experimental Data," CORROSION/2014, paper no. 4353 (Houston, TX, NACE, 2014).

6. P.K. Shukla and A. Nordquist, "A Simplified Model to Simulate Electrolytic Coupling in Cased Pipeline Crossings," CORROSION/2017, paper no. C2017-8974 (Houston, TX, NACE, 2017).

7. ISO 15589-1 (2003). "Petroleum and Natural Gas Industries-Cathodic Protection of Pipeline Transportation Systems-Part 1: On Liquid Pipelines." (International Standard Organization, Geneva, Switzerland).

8. P.K. Shukla, X. He, and A. Nordquist. "Applicability of Vapor Corrosion Inhibitors for Corrosion Mitigation in Pipeline Casings." Southwest Research Institute, March 2017.